Selected Paper

Syntheses, Crystal Structures, and Conversion of Three Linkage Isomers of Di-2-pyridyl Ketone in Dichlorobis(dimethyl sulfoxide-*S*)-ruthenium(II) and Chlorobis(dimethyl sulfoxide-*S*)ruthenium(II) Complexes: [$RuCl_2$(dpk-κ^2N,O)(dmso-S)$_2$], [$RuCl_2$(dpk-κ^2N,N')-(dmso-S)$_2$], and [RuCl(dpk-OH-κ^3N,O,N')(dmso-S)$_2$]

Mari Toyama,* Makito Nakahara, and Noriharu Nagao*

Department of Applied Chemistry, Meiji University, Kawasaki 214-8571

Received October 26, 2006; E-mail: nori@isc.meiji.ac.jp

The reaction between *trans*-[$RuCl_2$(dmso-S)$_4$] (dmso = dimethyl sulfoxide) and di-2-pyridyl ketone (dpk) in H_2O at room temperature afforded *trans*(Cl),*cis*(S)-[$RuCl_2$(dpk-κ^2N,O)(dmso-S)$_2$] (**1**) in high yield, while the reaction between *cis*(Cl),*fac*(S)-[$RuCl_2$(dmso-S)$_3$(dmso-O)] and dpk in EtOH–DMSO at reflux afforded *cis*(Cl),*cis*(S)-[$RuCl_2$-(dpk-κ^2N,N')(dmso-S)$_2$] (**2**). Reaction of **1** with Ag^+ and OH^- afforded the one-dimensional Ru–Ag coordination polymer *trans*(Cl),*cis*(S)-[$AgRuCl_2$(dpk-OH-κ^3N,O,N')(dmso-S)$_2$]$_n$ (**3**), which, as shown by X-ray crystallographic analysis, was in an "arrested" state of chloride ion abstraction. Reaction of **3** in DMSO afforded a mixture of two isomers containing dpk-OH-κ^3N,O,N': *trans*(Cl,O),*cis*(S)- and *cis*(Cl,O),*cis*(S)-[RuCl(dpk-OH-κ^3N,O,N')(dmso-S)$_2$] (**4a** and **4b**, respectively). The *trans*(Cl,O),*cis*(S)-isomer **4a** was selectively synthesized by reaction of **1** with OH^- in H_2O, while the *cis*(Cl,O),*cis*(S)-isomer **4b** was selectively synthesized by reaction of **2** with OH^- in H_2O. The isomerization reaction between **4a** and **4b** in DMSO solution was found to be reversible, and **4b** was favored over **4a**, with $K_{4ab} = [\mathbf{4b}]/[\mathbf{4a}] = 1.5 \pm 0.1$. The crystal structures of **1** and **2** showed that the geometry of the $RuCl_2$(dmso-S)$_2$ unit caused selective formation of the κ^2N,O- and κ^2N,N'-coordination modes of the dpk ligand. In **4a**, the flexibility of the κ^3N,O,N'-coordination mode of the (dpk-OH)$^-$ ligand mitigates the steric hindrance caused by the RuCl(dmso-S)$_2^+$ unit.

Ruthenium(II) complexes containing polypyridyl ligands have been investigated with much interest for their photochemical, electrochemical, and biochemical properties.[1–10] Most of the ruthenium(II) polypyridyl complexes that have hitherto been studied contain 2,2′-bipyridine (bpy), 1,10-phenanthroline (phen), or analogous ligands, which coordinate to a metal ion via two pyridyl N atoms to form a five-membered chelate ring.

Di-2-pyridyl ketone (dpk) has been used as polypyridyl ligand in a variety of the metal complexes, and several binding modes have been established for this ligand.[11–29] It can coordinate as a bidentate ligand to the metal ion via one of two modes: either through the two pyridyl N atoms (κ^2N,N'-coordination mode) or through one pyridyl N atom and a carbonyl O atom (κ^2N,O-coordination mode). However, in the majority of bidentate dpk complexes, the ligand is in the κ^2N,N'-coordination mode; the κ^2N,O-coordination mode is rare.[11,12] The κ^2N,O-coordination modes of dpk and its analogous ligands have attracted interest because of their possibly hemilabile nature, which is due to the presence of one strong *N*-donor and one weak *O*-donor. Complexes with this type of ligand are potential catalyst precursors.[30–32] With this in mind, ruthenium(II) complexes with 2-acetylpyridine (2-apy), 2-benzoylpyridine (2-bzpy), and other ligands containing a κ^2N,O 2-pyridyl ketone bonded moiety, which are analogous to dpk in the κ^2N,O-coordination mode, have been synthesized.[33–38] Pal and Pal have reported the synthesis and X-ray crystal structure of *trans*(Cl),*cis*(S)-[$RuCl_2$(2-apy)(dmso-S)$_2$] (dmso = dimethyl sulfoxide), which is produced by refluxing *trans*-[$RuCl_2$(dmso-S)$_4$][39] and 2-acetylpyridine in methanol.[33] In *trans*(Cl),*cis*(S)-[$RuCl_2$(2-apy)(dmso-S)$_2$], 2-acetylpyridine, which binds to the ruthenium ion through the pyridyl N and carbonyl O atoms to form a five-membered chelate ring, contains a κ^2N,O 2-pyridyl ketone bonded moiety. As far as we know, there are few X-ray crystal structures of ruthenium(II) complexes with a 2-benzoylpyridine ligand, which also acts as a bidentate ligand to the ruthenium ion via the pyridyl N and carbonyl O atoms.[34–38]

Furthermore, there is another possible coordination mode for dpk. Coordinated dpk frequently undergoes nucleophilic addition of water or an alcohol at the carbonyl carbon atom to form the diol or corresponding hemiacetal, $(NC_5H_4)_2C(OR)(OH)$, of which the deprotonated form $(NC_5H_4)_2C(OR)(O^-)$ acts as a mononegative tridentate N,O,N'-donor ligand (κ^3N,O,N'-coordination mode). There have been few reports on the conversion between κ^2N,N'- and κ^3N,O,N'-coordination modes.[13,14,28,29] Crowder and co-workers have reported the syntheses and crystal structures of two platinum complexes containing dpk in κ^2N,N'- or κ^3N,O,N'-coordination modes, [$PtCl_4$(dpk-κ^2N,N')] and [$PtCl_3$(dpk-OH-κ^3N,O,N')](Hphen)-Cl, the latter of which is obtained by reaction of [$PtCl_4$-(dpk-κ^2N,N')] with 1,10-phenanthroline (phen).[13] Bakir and McKenzie have reported that nucleophilic addition of water at the carbonyl C atom of the coordinate dpk in *fac*-[ReCl-

Published on the web May 14, 2007; doi:10.1246/bcsj.80.937

$(CO)_3$(dpk-κ^2N,N')] and *cis*-[ReCl$(CO)_2(PPh_3)$(dpk-κ^2N,N')] results in hydration of the keto groups and formation of *fac*-[Re$(CO)_3$(dpk-OH-κ^3N,O,N')] and *cis*-[Re$(CO)_2(PPh_3)$(dpk-OH-κ^3N,O,N')], respectively.[14]

No X-ray crystal structures of ruthenium(II) complexes with dpk, which binds to the ruthenium ion through the pyridyl N and carbonyl O atoms (κ^2N,O-coordination mode), have yet been reported. In all ruthenium(II) dpk complexes, of which the structures have been determined by X-ray crystallography, dpk acts as a bidentate N,N'-donor ligand or a tridentate N,O,N'-donor ligand.[15–20] There is only one report of an X-ray crystal structure of a bis(dpk-OH)ruthenium(II) complex, *trans*(O)-[Ru(dpk-OH-κ^3N,O,N')$_2$]$\cdot 8H_2O$.[20]

We have reported selective synthetic methods for *trans*(Cl),*cis*(S)-[$RuCl_2$(L-L)(dmso-*S*)$_2$] (L-L = 2,2′-bipyridine (bpy) or di-2-pyridylamine (Hdpa)) from *trans*-[$RuCl_2$(dmso-*S*)$_4$], and *cis*(Cl),*cis*(S)-[$RuCl_2$(bpy)(dmso-*S*)$_2$] from *cis*(Cl),-*fac*(S)-[$RuCl_2$(dmso-*S*)$_3$(dmso-*O*)].[40,41] Our methods for mono(polypyridine)ruthenium(II) complexes should also be applicable to mono(di-2-pyridyl ketone)ruthenium(II) complexes. In this paper, we report the synthesis and crystal structures of three types of mono(di-2-pyridyl ketone)ruthenium complexes: *trans*(Cl),*cis*(S)-[$RuCl_2$(dpk-κ^2N,O)(dmso-*S*)$_2$] (**1**), *cis*(Cl),*cis*(S)-[$RuCl_2$(dpk-κ^2N,N')(dmso-*S*)$_2$]$\cdot$DMSO (**2**$\cdot$DMSO), and *trans*(Cl),*cis*(S)-[AgRuCl_2(dpk-OH-κ^3N,O,N')-(dmso-*S*)$_2$]$_n$ (**3**).[42] We further report the conversion of dpk-κ^2N,O in **1** and dpk-κ^2N,N' in **2** into dpk-OH-κ^3N,O,N' in *trans*(Cl,O),*cis*(S)- and *cis*(Cl,O),*cis*(S)-[RuCl(dpk-OH-κ^3N,O,N')(dmso-*S*)$_2$] (**4a** and **4b**), respectively.[42]

Experimental

Hydrated ruthenium trichloride ($RuCl_3\cdot 3H_2O$) was purchased from Furuya Kinzoku Co. All other solvents and chemicals were of reagent quality and were used without further purification. The starting materials *cis*(Cl),*fac*(S)-[$RuCl_2$(dmso-*S*)$_3$(dmso-*O*)] and *trans*-[$RuCl_2$(dmso-*S*)$_4$] were prepared according to the literature.[39,43] All reactions were carried out under an argon atmosphere.

The ^{1}H (270 MHz) and ^{13}C (500 MHz) NMR spectra were recorded on a JEOL GSX-270 and an ECA-500 spectrometer at room temperature (298 K) unless otherwise noted. The aromatic signals of the ^{1}H NMR and of ^{13}C NMR spectra for the complexes were assigned on the basis of their coupling constants, ^{1}H–^{1}H COSY, ^{1}H–^{13}C HMQC, and ^{1}H–^{13}C HMBC experiments.

Kinetic studies were performed on the isomerization reaction between **4a** and **4b** using ^{1}H NMR spectroscopy in DMSO-d_6; kinetic data was obtained from successive ^{1}H NMR spectra. The intensities of selected signals were normalized with respect to a particular set of signals (usually the sum of the intensities of the H-6 signals for all species).

Synthesis of *trans*(Cl),*cis*(S)-[$RuCl_2$(dpk-κ^2N,O)(dmso-*S*)$_2$] (1). To a solution of *trans*-[$RuCl_2$(dmso-*S*)$_4$] (1.0 g, 2.1 mmol) in H_2O (20 mL) was added a solution of dpk (0.40 g, 2.2 mmol) in H_2O (10 mL). The mixture was stirred for 5 h at room temperature, during which a blue precipitate gradually appeared. The blue precipitate, *trans*(Cl),*cis*(S)-[$RuCl_2$(dpk-κ^2N,O)(dmso-*S*)$_2$] (**1**), was collected by filtration, washed with cold water and dried in vacuo (1.0 g, 95%). Blue crystals of **1** suitable for X-ray crystallography were obtained by vapor diffusion of diethyl ether into an acetonitrile solution of **1** at ca. 273 K. Anal. Calcd for $C_{15}H_{20}N_2Cl_2O_3S_2Ru$: C, 35.16; H, 3.93; N, 5.47%. Found: C, 35.18; H, 3.82; N, 5.55%. ^{1}H NMR (270 MHz, $CDCl_3$): δ 10.60 (1H, d, $J = 5.5$ Hz, H-6), 9.84 (1H, d, $J = 7.9$ Hz, H-3), 8.85 (1H, d, $J = 4.2$ Hz, H-6′), 8.24 (1H, d, $J = 8.0$ Hz, H-3′), 8.07 (1H, t, $J = 8.1$ Hz, H-4), 8.00 (1H, t, $J = 8.0$ Hz, H-4′), 7.84 (1H, dd, $J = 5.7$, 7.5 Hz, H-5), 7.64 (1H, dd, $J = 4.7$, 7.5 Hz, H-5′), 3.49 (6H, s, CH_3 of dmso), 3.43 (6H, s, CH_3 of dmso). ^{1}H NMR (270 MHz, DMSO-d_6): δ 10.36 (1H, d, $J = 5.5$ Hz, H-6), 9.63 (1H, d, $J = 7.8$ Hz, H-3), 8.94 (1H, d, $J = 4.7$ Hz, H-6′), 8.48 (1H, d, $J = 7.8$ Hz, H-3′), 8.34 (1H, t, $J = 7.8$ Hz, H-4), 8.22 (1H, t, $J = 7.8$ Hz, H-4′), 8.10 (1H, dd, $J = 5.5$, 7.8 Hz, H-5), 7.88 (1H, dd, $J = 4.7$, 7.8 Hz, H-5′), 3.49 (6H, s, CH_3 of dmso), 3.43 (6H, s, CH_3 of dmso). ^{13}C{^{1}H} NMR (500 MHz, $CDCl_3$): δ 199.4 (C=O), 156.3 (C-6), 152.3 (C-2′), 152.2 (C-2), 149.1 (C-6′), 137.7 (C-4′), 137.5 (C-4), 135.0 (C-3), 130.2 (C-5), 128.2 (C-5′), 126.5 (C-3′), 45.76 (CH_3 of dmso), 45.57 (CH_3 of dmso). ^{13}C{^{1}H} NMR (500 MHz, DMSO-d_6): δ 199.1 (C=O), 155.4 (C-6), 151.5 (C-2), 151.4 (C-2′), 149.4 (C-6′), 138.7 (C-4′), 138.4 (C-4), 134.7 (C-3), 130.3 (C-5), 129.0 (C-5′), 127.0 (C-3′), 44.99 (CH_3 of dmso), 44.81 (CH_3 of dmso).

Synthesis of *cis*(Cl),*cis*(S)-[$RuCl_2$(dpk-κ^2N,N')(dmso-*S*)$_2$]$\cdot$DMSO (2$\cdot$DMSO). A solution of *cis*(Cl),*fac*(S)-[$RuCl_2$(dmso-*S*)$_3$(dmso-*O*)] (500 mg, 1 mmol) and dpk (200 mg, 1.1 mmol) in EtOH (3 mL) and DMSO (3 mL) was refluxed for 1.5 h. While refluxing, the originally blue solution gradually turned brown, and small amounts of a red precipitate appeared. Nine mL of EtOH was then added, and the solution was refluxed again for 1.5 h. The red precipitate, *cis*(Cl),*cis*(S)-[$RuCl_2$(dpk-κ^2N,N')(dmso-*S*)$_2$]$\cdot$DMSO (**2**$\cdot$DMSO), that gradually appeared was collected by filtration, washed with cold EtOH, and dried in vacuo (380 mg, 73%). Red crystals of **2**$\cdot$DMSO suitable for X-ray crystallography were obtained by vapor diffusion of EtOH into a DMSO solution of **2**. While crystallizing, DMSO (1 molecule) was incorporated into the unit cell of the crystal of **2**$\cdot$DMSO. Anal. Calcd for $C_{15}H_{20}N_2Cl_2O_3S_2Ru\cdot(CH_3)_2SO$: C, 34.57; H, 4.44; N, 4.74%. Found: C, 34.45; H, 4.36; N, 4.72%. ^{1}H NMR (270 MHz, $CDCl_3$): δ 9.63 (1H, d, $J = 5.8$ Hz, H-6), 9.45 (1H, d, $J = 5.8$ Hz, H-6′), 8.35 (1H, d, $J = 7.7$ Hz, H-3′), 8.27 (1H, d, $J = 7.7$ Hz, H-3), 8.04 (1H, t, $J = 7.7$ Hz, H-4′), 8.00 (1H, t, $J = 7.7$ Hz, H-4), 7.56 (1H, dd, $J = 5.8$, 7.7 Hz, H-5′), 7.47 (1H, dd, $J = 5.8$, 7.7 Hz, H-5), 3.57 (3H, s, CH_3 of dmso), 3.50 (3H, s, CH_3 of dmso), 3.27 (3H, s, CH_3 of dmso), 2.90 (3H, s, CH_3 of dmso). ^{1}H NMR (270 MHz, DMSO-d_6): δ 9.44 (1H, d, $J = 6.0$ Hz, H-6), 9.07 (1H, d, $J = 5.7$ Hz, H-6′), 8.25 (2H, m, H-3′, H-4′), 8.12 (2H, m, H-3, H-4), 7.72 (1H, t, $J = 5.3$ Hz, H-5′), 7.58 (1H, t, $J = 6.0$ Hz, H-5), 3.50 (3H, s, CH_3 of dmso), 3.43 (3H, s, CH_3 of dmso), 3.25 (3H, s, CH_3 of dmso). ^{13}C{^{1}H} NMR (500 MHz, DMSO-d_6): δ 181.6 (C=O), 158.9 (C-6), 156.6 (C-2), 155.9 (C-6′), 155.1 (C-2′), 139.0 (C-4′), 138.1 (C-4), 127.2 (C-3), 127.0 (C-5′), 126.9 (C-3′), 125.1 (C-5), 45.74 (CH_3 of dmso), 45.22 (CH_3 of dmso), 45.17 (CH_3 of dmso), 44.52 (CH_3 of dmso).

Synthesis of *trans*(Cl),*cis*(S)-[AgRuCl_2(dpk-OH-κ^3N,O,N')-(dmso-*S*)$_2$]$_n$ (3). To a solution of **1** (100 mg, 0.20 mmol) in an aqueous solution of 0.1 M HOTf (150 mL), a stoichiometric amount of Ag(OTf) (57 mg, 0.22 mmol) was added. After stirring for 15 min, a 4 M aqueous solution of NaOH was added dropwise to the blue solution to neutralize the mixture. At pH 7, the solution turned from blue to yellow. A small amount of NaOH aqueous solution was then added to the yellow solution until it became slightly basic (pH 8–9). While stirring, a yellow precipitate rapidly appeared. The yellow precipitate, *trans*(Cl),*cis*(S)-[AgRuCl_2(dpk-OH-κ^3N,O,N')(dmso-*S*)$_2$]$_n$ (**3**), was collected by filtration, washed

with large amounts of water, and dried in vacuo (100 mg, 80%). Yellow crystals of **3** suitable for X-ray crystallography were grown over three days from a solution of **1** (50 mg, 0.1 mmol) in H_2O (20 mL) containing a stoichiometric amount of Ag(OTf) (23.5 mg, 0.1 mmol) at room temperature without stirring. Anal. Calcd for $C_{15}H_{21}N_2Cl_2O_4S_2RuAg$: C, 28.26; H, 3.32; N, 4.40%. Found: C, 28.26; H, 3.30; N, 4.33%. ^{1}H NMR (270 MHz, DMSO-d_6): δ 10.06 (1H, d, $J = 5.8$ Hz, H-6), 8.42 (1H, d, $J = 4.8$ Hz, H-6′), 8.20 (1H, d, $J = 7.6$ Hz, H-3′), 8.06 (1H, t, $J = 7.6$ Hz, H-4′), 7.64 (1H, t, $J = 7.4$ Hz, H-4), 7.52 (1H, dd, $J = 4.8, 7.6$ Hz, H-5′), 7.34 (1H, dd, $J = 5.8, 7.4$ Hz, H-5), 6.48 (1H, d, $J = 7.4$ Hz, H-3), 5.89 (1H, s, OH), 3.38 (3H, s, CH_3 of dmso), 3.29 (3H, s, CH_3 of dmso), 3.27 (3H, s, CH_3 of dmso), 3.22 (3H, s, CH_3 of dmso).

Synthesis of *trans*(Cl,O),*cis*(S)-[RuCl(dpk-OH-κ^3N,O,N')-(dmso-*S*)$_2$] (4a). To a suspension of **1** (150 mg, 0.3 mmol) in water (9.7 mL) was added 0.3 mL of a 1 M aqueous solution of LiOH, during which the blue suspension became a homogeneous orange solution. The reaction solution was stirred for 4 h at room temperature, and the solution turned yellow. After stirring for another 1 h (a total period of 5 h), the solution was evaporated to dryness under vacuum, and the residue was suspended EtOH (3 mL) to remove LiCl and LiOH. The yellow solid, *trans*(Cl,O),*cis*(S)-[RuCl(dpk-OH-κ^3N,O,N')(dmso-*S*)$_2$] (**4a**), was collected by filtration, washed with cold EtOH, and dried in vacuo (130 mg, 86%). Yellow crystals of **4a** suitable for X-ray crystallography were obtained by vapor diffusion of diethyl ether into an EtOH solution of **4a**. Anal. Calcd for $C_{15}H_{21}N_2ClO_4S_2Ru$: C, 36.47; H, 4.28; N, 5.67%. Found: C, 36.37; H, 4.33; N, 5.58%. ^{1}H NMR (270 MHz, DMSO-d_6): δ 8.84 (2H, d, $J = 5.4$ Hz, H-6), 7.88 (2H, t, $J = 7.64$ Hz, H-4), 7.59 (2H, d, $J = 7.7$ Hz, H-3), 7.42 (1H, s, OH), 7.34 (2H, dd, $J = 7.4, 5.6$ Hz, H-5), 3.12 (6H, s, CH_3 of dmso), 2.87 (6H, s, CH_3 of dmso). ^{13}C{^{1}H} NMR (500 MHz, DMSO-d_6): δ 166.8 (C-2), 152.5 (C-6), 137.7 (C-4), 122.5 (C-5), 119.5 (C-3), 102.7 (HO–C–O$^-$ of the gem-diol), 43.85 (CH_3 of dmso), 43.39 (CH_3 of dmso).

Synthesis of *cis*(Cl,O),*cis*(S)-[RuCl(dpk-OH-κ^3N,O,N')-(dmso-*S*)$_2$] (4b). Method A: To a suspension of **2** (150 mg, 0.3 mmol) in water (40 mL) was added 10 mL of a 5 M aqueous solution of LiOH. While stirring at room temperature for 1.5 h, the red suspension gradually became an almost homogeneous yellow solution. After stirring for another 1 h (a total period of 2.5 h), the resulting solution was filtered to remove a small amount of insoluble matter. An aqueous solution of HCl (6 M) was then added dropwise to the filtrate until the mixture was just neutral, and the solution was evaporated to approximately 5 mL under vacuum. While evaporating, a yellow precipitate, *cis*(Cl,O),*cis*(S)-[RuCl-(dpk-OH-κ^3N,O,N')(dmso-*S*)$_2$] (**4b**), gradually appeared. This was collected by filtration, washed with cold H_2O, and dried in vacuo (100 mg, 66%). Anal. Calcd for $C_{15}H_{21}N_2ClO_4S_2Ru\cdot 0.5H_2O$: C, 35.74; H, 4.11; N, 5.54%. Found: C, 35.81; H, 4.40; N, 5.57%. ^{1}H NMR (270 MHz, DMSO-d_6): δ 8.95 (1H, d, $J = 5.7$ Hz, H-6), 8.72 (1H, d, $J = 5.3$ Hz, H-6′), 7.90 (1H, t, $J = 7.7$ Hz, H-4′), 7.82 (1H, t, $J = 7.5$ Hz, H-4), 7.69 (1H, d, $J = 7.7$ Hz, H-3′), 7.62 (1H, d, $J = 7.5$ Hz, H-3), 7.57 (1H, s, OH), 7.34 (1H, dd, $J = 5.3, 7.7$ Hz, H-5′), 7.26 (1H, dd, $J = 5.7, 7.5$ Hz, H-5), 3.40 (3H, s, CH_3 of dmso), 3.01 (3H, s, CH_3 of dmso), 2.99 (3H, s, CH_3 of dmso).

Method B: A suspension of **4a** (150 mg, 0.3 mmol) in DMSO (4.5 mL) was heated to 373 K for 5 h. While heating, the yellow suspension gradually became homogeneous (after ca. 1.5 h), followed by gradual appearance of a yellow precipitate. After the reaction mixture had been cooled to room temperature, water was added to the reaction solution in sufficient amounts (6 mL) to precipitate the product. The yellow precipitate was collected by filtration, washed with water and then with EtOH, and dried in vacuo (80 mg, 55%).

X-ray Crystallography. Data for all crystals were collected using the ω-2θ scan technique ($2\theta < 55^\circ$) on a Rigaku AFC-7R automated four-circle X-ray diffractometer equipped with graphite-monochromatized Mo Kα radiation ($\lambda = 0.71069$ Å) at 296 K. All calculations were carried out on an O_2 workstation (SGI) using the teXsan crystallographic software package.[44] The structures were solved by the direct method and expanded using Fourier techniques. The non-hydrogen atoms were refined anisotropically. Hydrogen atoms were positioned in idealized positions and included in the structure factor calculations. For **2**, disordered DMSO (1 molecule) was included at a general position, which was modeled by two-site positional disorder. The hydrogen atoms of disordered solvent DMSO were not included in the structure factor calculation. The crystallographic data for **1**, **2**·DMSO, **3**, and **4a** are summarized in Table 1.

Crystallographic data have been deposited with Cambridge Crystallographic Data Centre: Deposition numbers CCDC-629116–629119 for compound Nos. **1**, **2**·DMSO, **3**, and **4a**, respectively. Copies of the data can be obtained free of charge via http://www.ccdc.cam.ac.uk/conts/retrieving.html (or from the Cambridge Crystallographic Data Centre, 12, Union Road, Cambridge, CB2 1EZ, UK; Fax: +44 1223 336033; e-mail: deposit@ccdc.cam.ac.uk).

Results and Discussion

Syntheses and Characterization of *trans*(Cl),*cis*(S)-[RuCl$_2$(dpk-κ^2N,O)(dmso-*S*)$_2$] (1) and *cis*(Cl),*cis*(S)-[RuCl$_2$(dpk-κ^2N,N')(dmso-*S*)$_2$] (2). The reaction of *trans*-[RuCl$_2$(dmso-*S*)$_4$] with L-L ligands (L-L = bpy or Hdpa) at 273 K affords only *trans*(Cl),*cis*(S)-[RuCl$_2$(L-L)(dmso-*S*)$_2$], which precipitate spontaneously from the reaction mixture.[40,41] In case of the dpk ligand, the reaction could be carried out at room temperature and for a shorter reaction time than for the bpy and Hdpa ligands. The reaction of *trans*-[RuCl$_2$(dmso-*S*)$_4$] with dpk ligand at room temperature afforded only **1** in high yield (≈95%), and spontaneous precipitation of **1** allowed for convenient collection without further purification. However, complex **1** was blue (Fig. S1), in contrast to the analogous complexes *trans*(Cl),*cis*(S)-[RuCl$_2$(L-L)(dmso-*S*)$_2$], which are yellow or red.

The ^{1}H NMR spectrum of **1** in DMSO-d_6 is shown in Fig. 1. Eight signals with intensities of 1H can be seen in the aromatic region and two singlets with intensities of 6H can be seen in the aliphatic region. The intensities of the signals indicate that **1** possesses one dpk and two dmso ligands. The spectral pattern of **1** indicates that the two pyridine rings of the dpk ligand are not equivalent. This is in contrast to *trans*(Cl),*cis*(S)-[RuCl$_2$(L-L)(dmso-*S*)$_2$], in which two pyridine rings of the L-L ligand are equivalent. The color and ^{1}H NMR spectrum of **1** suggest that **1** possesses an unusual structure; this was confirmed by X-ray crystal analysis.

An ORTEP drawing of **1** is shown in Fig. 2. The Ru ion had a distorted octahedral geometry with two *trans*(Cl) atoms (*trans*(Cl),*cis*(S)-isomer), and the dpk ligand coordinated through a pyridyl N atom and a carbonyl O atom. During the reaction, two dmso ligands of *trans*-[RuCl$_2$(dmso-*S*)$_4$] were substituted by a dpk ligand to afford the mono(di-2-pyridyl

Table 1. Crystallographic Data for **1**, **2**·DMSO, **3**, and **4a**

	1	**2**·DMSO	**3**	**4a**
Experimental formula	$RuCl_2C_{15}N_2S_2O_3H_{20}$	$RuCl_2C_{17}N_2S_3O_4H_{26}$	$RuAgCl_2C_{15}N_2S_2O_4H_{21}$	$RuClC_{15}N_2S_2O_4H_{21}$
Formula weight	512.43	590.56	637.31	493.98
Crystal system	monoclinic	monoclinic	monoclinic	monoclinic
Space group	$P2_1/a$ (# 14)	$P2_1/n$ (# 14)	$P2_1/n$ (# 14)	$P2_1/n$ (# 14)
Lattice parameters				
a/Å	17.235(4)	17.656(2)	20.679(6)	14.710(4)
b/Å	8.595(2)	8.4507(6)	7.534(3)	15.911(7)
c/Å	14.738(4)	15.811(2)	14.278(4)	8.440(4)
α/°	90	90	90	90
β/°	115.00(2)	93.236(8)	107.99(2)	97.87(3)
γ/°	90	90	90	90
V/Å^3	1978.8(9)	2355.5(4)	2115(1)	1956(1)
Z	4	4	4	4
D_{calcd}/g cm^{-3}	1.720	1.665	2.001	1.677
F_{000}	1032.00	1200.00	1256.00	1000.00
μ (Mo Kα)/cm^{-1}	12.90	11.84	19.90	11.73
Independent reflection	4540	5400	4855	4490
Data to parameter ratio	20.00	19.85	19.90	19.87
$R1$ [$I > 2\sigma(I)$]/No. of reflection	0.030/3702	0.040/4703	0.025/3966	0.028/3655
$wR2$ (all data)	0.096/4540	0.115/5400	0.088/4855	0.088/4490
GOF	1.30	1.68	1.14	1.13

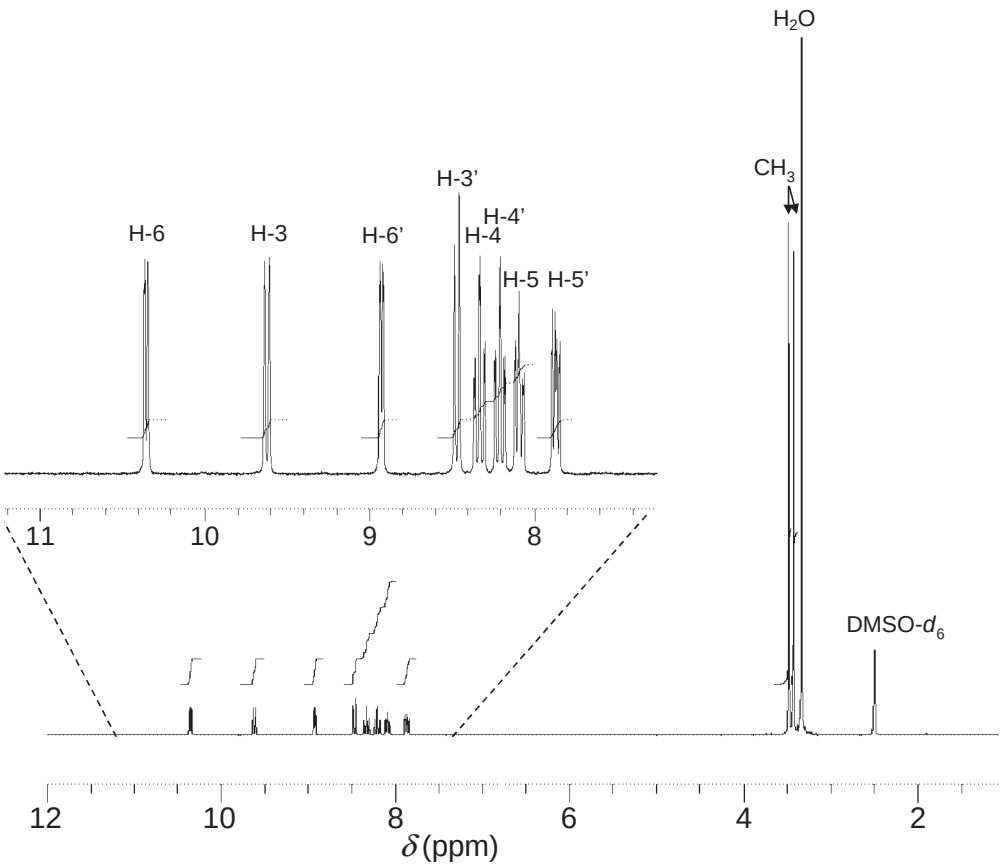

Fig. 1. ^{1}H NMR spectrum of **1** in DMSO-d_6. Spectrum was recorded at room temperature (298 K).

ketone)ruthenium(II) complex *trans*(Cl),*cis*(S)-[$RuCl_2$(dpk-κ^2N,O)(dmso-S)$_2$], in which the *trans*(Cl)-configuration of the starting material was retained (Scheme 1). The *trans*(Cl),-*cis*(S)-configuration of two dmso and two Cl^- ligands in **1** was the same as that of the analogous *trans*(Cl),*cis*(S)-[$RuCl_2$(L-L)(dmso-S)$_2$], although there was a difference in the coordina-

tion mode of dpk.

Here, in accordance with the X-ray crystal structure, the assignments of the aromatic signals in the ^{1}H NMR spectrum of **1** were done by using coupling constants and ^{1}H–^{1}H COSY experiments. The chemical shifts of H-3, H-4, H-5, and H-6 signals, which were assigned to one pyridine ring, were downfield compared to those of H-3′, H-4′, H-5′, and H-6′ signals, respectively, which were assigned to another pyridine ring. Therefore, the pyridine ring with H-3–H-6 could be assigned to the coordinate pyridyl-N(1) group.

In the case of the analogous bpy and Hdpa complexes, the *trans*(Cl),*cis*(S)-isomer is converted to the *cis*(Cl),*cis*(S)-isomer in DMSO solution.[40,41] When the *trans*(Cl),*cis*(S)-isomer **1** was dissolved in DMSO or acetonitrile, the κ^2N,O-dpk ligand dissociated to yield free dpk ligand, and no other geometrical or linkage isomers (*cis*(Cl),*cis*(S)-isomer or κ^2N,N'-isomer) were obtained (Fig. S2). Ruthenium(II) complexes with 2-benzoylpyridine and its derivative ligands, which contain a κ^2N,O 2-pyridyl ketone moiety, also dissociate in acetonitrile to yield free ligands.[34] The ligand dissociation reactions of these complexes in DMSO or acetonitrile may be due to the hemilabile nature of κ^2N,O coordinate ligands. It is notable that the labile (hemilabile) complex with κ^2N,O-dpk could be selectively synthesized in high yield.

We have reported that the reaction of *cis*(Cl),*fac*(S)-[$RuCl_2$(dmso-*S*)$_3$(dmso-*O*)] with bpy in EtOH–DMSO (9:1) selectively affords *cis*(Cl),*cis*(S)-[$RuCl_2$(bpy)(dmso-*S*)$_2$] in good yield.[40] In order to prepare another isomer (*cis*(Cl),*cis*(S)), the dpk ligand was reacted with *cis*(Cl),*fac*(S)-[$RuCl_2$(dmso-*S*)$_3$(dmso-*O*)] in EtOH–DMSO (1:1). The reaction mixture turned blue in the initial stage, which suggested that the species with κ^2N,O-dpk formed. Although attempts to isolate the blue species were unsuccessful, the reaction mixture turned brown when heat was maintained, and red *cis*(Cl),*cis*(S)-[$RuCl_2$(dpk-κ^2N,N')(dmso-*S*)$_2$] (**2**) gradually precipitated (Scheme 1). This suggests that the κ^2N,O-coordination mode of dpk is kinetically favorable due to the small O donor atom of the carbonyl group, but the κ^2N,N'-coordination mode is more thermodynamically stable. Even though the *cis*(Cl),*cis*(S)-isomer **2** in DMSO solution was heated at 323 K for 16 h, the κ^2N,N'-dpk ligand did not dissociate, and no other geometrical or linkage isomers were formed (Fig. S3).

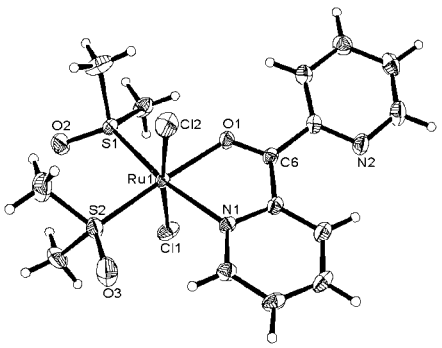

Fig. 2. ORTEP drawing of **1** with 30% probability ellipsoids.

The ^{1}H NMR spectrum of **2** in DMSO-d_6 exhibited four signals with intensities of 1H and two signals with intensities of 2H in the aromatic region, and three signals with intensities of 3H in the aliphatic region (Fig. S4). The spectral pattern indicates that the two pyridine rings of the κ^2N,N'-coordinate dpk ligand are in different environments. Therefore, the Cl^- and dmso ligands occupy *trans* positions to the dpk ligand (*cis*(Cl),*cis*(S)-isomer), which means that **2** is a geometrical and linkage isomer of **1**. The aromatic signals were assigned on the basis of their coupling constants and ^{1}H–^{1}H COSY experiment. Although only three methyl signals out of four were observed in DMSO-d_6, four methyl signals were observed in $CDCl_3$ (δ 3.57, 3.50, 3.27, and 2.90), which means that the remaining methyl signal in DMSO-d_6 was obscured by the H_2O signal at δ 3.33. In the $CDCl_3$ spectrum, the H_2O signal appeared at δ 1.57 (Fig. S5).

An ORTEP drawing of **2**·DMSO is shown in Fig. 3. The X-ray crystal structure showed that the geometry of **2** agreed with that of the *cis*(Cl),*cis*(S)-isomer proposed based on the ^{1}H NMR spectrum. The Ru ion had a distorted octahedral geometry with the Cl atom *trans* to the S atom of the dmso ligand (*cis*(Cl),*cis*(S)-isomer) and the dpk ligand coordinated as a bidentate ligand through two pyridyl N atoms (κ^2N,N').

Crystal Structures of 1 and 2. Selected bond lengths and angles of **1** and **2** are listed in Tables 2 and 3, respectively. The bond parameters of **1** were consistent with those of *trans*-(Cl),*cis*(S)-[$RuCl_2$(2-apy-κ^2N,O)(dmso-*S*)$_2$] (2-apy = 2-acetylpyridine); the non-coordinate pyridyl group in the former and the methyl group in the latter did not have a significant influence on the structure of the Ru coordination sphere.

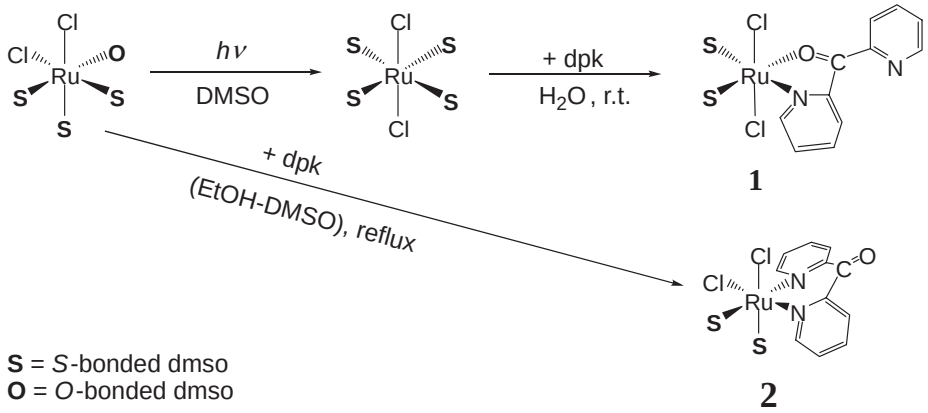

Scheme 1.

The five-membered chelate ring Ru(1)–N(1)–C(1)–C(6)–O(1) was approximately coplanar with the equatorial dmso ligands. The sum of the three angles around the carbonyl carbon atom C(6) was 359.8(6)°, and the C(6) maintained its sp^2 hybridization geometry. The C(6)–O(1) distance (1.243(3) Å) was longer than those found in ruthenium complexes with dpk-κ^2N,N' (1.178–1.221 Å),[17–19] which are comparable to the reported double bond values. This indicates that the bond interaction between the Ru^{2+} ion and the carbonyl O atom involves not only σ-donation but also π back-donation to π^*-orbital of carbonyl group.

The most interesting feature of the structure of **1** is the coordination mode of the dpk ligand. Although a dpk ligand can coordinate through two pyridyl N atoms, similarly to an Hdpa ligand, the dpk ligand acts as a bidentate ligand, coordinating through a pyridyl nitrogen atom, N(1), and a carbonyl oxygen atom, O(1). Selectivity towards the rare κ^2N,O-coordination mode of the dpk ligand in the reaction of *trans*-[$RuCl_2$(dmso-*S*)$_4$] with dpk ligand was very high (yield ≈95%), and no complex with a different coordination mode (κ^2N,N') was obtained under these reaction conditions. This high selectivity is caused by the steric effect of the two dmso ligands in the equatorial plane. The Ru–S distances (av. 2.245 Å) were shorter than those of *trans*(Cl),*cis*(S)-[$RuCl_2$(bpy)(dmso-*S*)$_2$] (av. 2.291 Å) and *trans*(Cl),*cis*(S)-[$RuCl_2$(Hdpa)(dmso-*S*)$_2$] (av. 2.277 Å). The equatorial Ru–S distances also suggest a decrease in steric hindrance among equatorial ligands in **1** compared to the analogous bpy and Hdpa complexes. The Ru(1)–N(1) distance (2.113(2) Å) was slightly shorter than those of the analogous bpy and Hdpa complexes *trans*(Cl),*cis*(S)-[$RuCl_2$(L-L)(dmso-*S*)$_2$] (2.123(4)–2.131(4) Å), in which the longer Ru–N distance was attributed to the steric effect of *cis* dmso ligands within the equatorial plane rather than the *trans* influence of the dmso ligand.[40,41] Therefore, the steric effect of the two dmso ligands in the equatorial plane results in a preference for the sterically slim κ^2N,O-coodination mode and prevents adoption of the bulky κ^2N,N'-coodination mode.

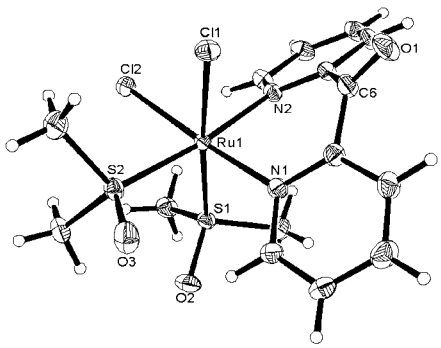

Fig. 3. ORTEP drawing of **2**·DMSO with 30% probability ellipsoids. The DMSO molecule is omitted for clarity.

The Ru–Cl and Ru–S distances in **2** were comparable to the corresponding distances in the analogous Hdpa complex *cis*(Cl),*cis*(S)-[$RuCl_2$(Hdpa)(dmso-*S*)$_2$], which has the same *cis*(Cl),*cis*(S)-geometry and six-membered chelate ring as **2**.[41] The Ru–N bond distances agreed with reported data on [Ru(terpy)(dpk-κ^2N,N')X]$^{n+}$ (terpy = 2,2′:6′,2″-terpyridine; X = Cl^-, CH_3CN, NO_2^-, and NO^+).[17] The dihedral angle of two pyridine rings of the dpk ligand was 44.5(1)°, which was also similar to those of [Ru(terpy)(dpk-κ^2N,N')X]$^{n+}$ (41.67–46.04°).[17]

Table 2. Selected Bond Lengths (Å) for **1**, **2**·DMSO, **3**, and **4a**

	trans[a)]	**1**	**2**·DMSO	**3**	**4a**
Ru–N bond					
	Cl		Ru(1)–N(1), 2.098(3)	Ru(1)–N(1), 2.125(3)	
	S	Ru(1)–N(1), 2.113(2)			Ru(1)–N(1), 2.096(2)
			Ru(1)–N(2), 2.114(2)		Ru(1)–N(2), 2.093(2)
Ru–Cl bond					
	Cl	Ru(1)–Cl(1), 2.397(1)		Ru(1)–Cl(1), 2.420(1)	
		Ru(1)–Cl(2), 2.391(1)		Ru(1)–Cl(2), 2.400(1)	
	S		Ru(1)–Cl(1), 2.429(1)		
	N		Ru(1)–Cl(2), 2.416(1)		
	O				Ru(1)–Cl(1), 2.413(1)
Ru–S bond					
	Cl		Ru(1)–S(1), 2.240(1)		
	N	Ru(1)–S(1), 2.252(1)	Ru(1)–S(2), 2.320(1)	Ru(1)–S(1), 2.256(1)	Ru(1)–S(1), 2.269(1)
					Ru(1)–S(2), 2.244(1)
	O	Ru(1)–S(2), 2.238(1)		Ru(1)–S(2), 2.247(1)	
Ru–O bond					
	N	Ru(1)–O(1), 2.089(2)		Ru(1)–O(1), 2.105(2)	
	Cl				Ru(1)–O(1), 2.094(2)
C–O bond		C(6)–O(1), 1.243(3)	C(6)–O(1), 1.209(4)	C(6)–O(1), 1.367(3)	C(6)–O(1), 1.403(3)
				C(6)–O(2), 1.441(4)	C(6)–O(2), 1.387(3)

a) Coordinate atom in *trans* position.

Table 3. Selected Bond Angles (°) for **1**, **2**·DMSO, **3**, and **4a**

1		**2**·DMSO		**3**		**4a**	
Axial							
Cl(1)–Ru(1)–Cl(2),	173.88(3)	Cl(1)–Ru(1)–S(1),	175.28(3)	Cl(1)–Ru(1)–Cl(2),	176.74(3)	Cl(1)–Ru(1)–O(1),	168.91(5)
Axial–Equatorial							
Cl(1)–Ru(1)–N(1),	86.58(6)	Cl(1)–Ru(1)–N(1),	86.15(7)	Cl(1)–Ru(1)–N(1),	87.78(7)	Cl(1)–Ru(1)–N(1),	92.73(6)
Cl(1)–Ru(1)–O(1),	88.41(6)	Cl(1)–Ru(1)–N(2),	85.84(7)	Cl(1)–Ru(1)–O(1),	90.83(6)	Cl(1)–Ru(1)–N(2),	93.96(7)
Cl(1)–Ru(1)–S(1),	89.66(3)	Cl(1)–Ru(1)–Cl(2),	90.79(3)	Cl(1)–Ru(1)–S(1),	92.62(3)	Cl(1)–Ru(1)–S(1),	88.76(3)
Cl(1)–Ru(1)–S(2),	93.82(4)	Cl(1)–Ru(1)–S(2),	89.27(3)	Cl(1)–Ru(1)–S(2),	90.90(3)	Cl(1)–Ru(1)–S(2),	94.60(3)
Cl(2)–Ru(1)–N(1),	86.58(6)	S(1)–Ru(1)–N(1),	89.35(7)	Cl(2)–Ru(1)–N(1),	89.10(7)	O(1)–Ru(1)–N(1),	78.67(8)
Cl(2)–Ru(1)–O(1),	87.13(6)	S(1)–Ru(1)–N(2),	92.62(7)	Cl(2)–Ru(1)–O(1),	87.55(6)	O(1)–Ru(1)–N(2),	78.05(8)
Cl(2)–Ru(1)–S(1),	90.30(4)	S(1)–Ru(1)–Cl(2),	93.66(3)	Cl(2)–Ru(1)–S(1),	90.25(3)	O(1)–Ru(1)–S(1),	99.01(5)
Cl(2)–Ru(1)–S(2),	87.28(5)	S(1)–Ru(1)–S(2),	92.59(3)	Cl(2)–Ru(1)–S(2),	90.52(3)	O(1)–Ru(1)–S(2),	92.84(6)
Equatorial							
N(1)–Ru(1)–O(1),	76.12(8)	N(1)–Ru(1)–N(2),	88.6(1)	N(1)–Ru(1)–O(1),	77.39(9)	N(1)–Ru(1)–N(2),	82.12(9)
S(1)–Ru(1)–S(2),	93.41(3)	Cl(2)–Ru(1)–S(2),	86.48(3)	S(1)–Ru(1)–S(2),	92.69(3)	S(1)–Ru(1)–S(2),	93.40(3)
N(1)–Ru(1)–S(2),	93.41(3)	N(1)–Ru(1)–S(2),	95.31(8)	N(1)–Ru(1)–S(2),	98.66(7)	N(1)–Ru(1)–S(2),	92.93(7)
O(1)–Ru(1)–S(1),	91.11(5)	N(2)–Ru(1)–Cl(2),	89.30(7)	O(1)–Ru(1)–S(1),	91.25(6)	N(2)–Ru(1)–S(1),	91.33(6)
Around C(6) atom of ketone							
C(1)–C(6)–C(7),	125.8(2)	C(1)–C(6)–C(7),	119.6(3)	C(1)–C(6)–C(7),	109.2(2)	C(1)–C(6)–C(7),	106.1(2)
O(1)–C(6)–C(1),	117.1(2)	O(1)–C(6)–C(1),	119.4(3)	O(1)–C(6)–C(1),	110.4(2)	O(1)–C(6)–C(1),	108.4(2)
O(1)–C(6)–C(7),	116.9(2)	O(1)–C(6)–C(7),	119.6(3)	O(1)–C(6)–C(7),	112.1(2)	O(1)–C(6)–C(7),	107.0(2)
Dihedral angle[a)]							
Plane(1)–Plane(2),	16.4(1)	Plane(1)–Plane(2),	44.5(1)	Plane(1)–Plane(2),	88.8(1)	Plane(1)–Plane(2),	74.4(1)

a) Plane(1) = N(1), C(1), C(2), C(3), C(4), C(5); Plane(2) = N(2), C(7), C(8), C(9), C(10), C(11).

The six-membered chelate ring Ru(1)–N(1)–C(1)–C(6)–C(7)–N(2) adopted a boat conformation, with the Ru(1) and C(6) atoms 0.759 and 0.413 Å, respectively, below the plane defined by the remaining four atoms. The C(6)–O(1) distance (1.209(4) Å) was comparable to the reported double bond values.[17–19] The three angles around the carbonyl carbon atom C(6) were nearly 120°, and the C(6) had an ideal sp^2 hybridization geometry. The N(1)–Ru(1)–N(2) bite angle of 88.6(1)° was close to the ideal angle (90°) in the octahedral geometry. These angles indicate that the dpk-κ^2N,N' ligand does not suffer serious steric effects from the *cis*(Cl),*cis*(S)-Cl_2(dmso-*S*)$_2$ co-ligands. In the analogous Hdpa complexes [$RuCl_2$(Hdpa)(dmso-*S*)$_2$], the *cis*(Cl),*cis*(S)-geometry has a smaller steric effect than *trans*(Cl),*cis*(S)-geometry.[41] Therefore, the smaller steric effect of *cis*(Cl),*cis*(S)-Cl_2(dmso-*S*)$_2$ co-ligands in **2** results in a preference for the κ^2N,N'-coordination mode of the dpk ligand. In contrast, the sterically hindering *trans*(Cl),*cis*(S)-Cl_2(dmso-*S*)$_2$ co-ligands in **1** prevent adoption of the κ^2N,N'-coordination mode of dpk, resulting in adoption of the κ^2N,O-coordination mode (Scheme 1).

Synthesis and Structure of *trans*(Cl),*cis*(S)-[AgRuCl$_2$(dpk-OH-κ^3N,O,N')(dmso-*S*)$_2$]$_n$ (3). To overcome the problem of hemilability in **1**, another synthetic methodology was developed. Thus, the reaction of **1** with Ag^+ was attempted with the aim of abstracting a Cl^- ligand from the $RuCl_2$(dmso-*S*)$_2$ unit to afford a RuCl(dmso-*S*)$_2^+$ cation unit. A 50 mg (0.1 mmol) sample of **1** was dissolved in 20 mL of water and then one equiv of Ag(OTf) (23.5 mg, 0.1 mmol) was added. Although the reaction mixture was allowed to stand at room temperature for several hours, it was noted that no AgCl precipitate formed. After three days, yellow crystals were deposited without AgCl precipitation (11 mg, 17%). X-ray analysis of the yellow crystals revealed that the reaction of **1** with Ag^+ afforded the one-dimensional Ru–Ag coordination polymer *trans*(Cl),*cis*(S)-[AgRuCl$_2$(dpk-OH-κ^3N,O,N')(dmso-*S*)$_2$]$_n$ (**3**) rather than the desired product.

An ORTEP drawing of **3** is shown in Fig. 4, and selected bond lengths and angles are listed in Tables 2 and 3, respectively. The Ru ion had a distorted octahedral geometry with two *trans*(Cl) atoms and two *cis*(S) atoms from the dmso ligands (*trans*(Cl),*cis*(S)-isomer), which was comparable to the geometry of **1**; however, the coordination mode of the dpk ligand in **3** was different from that of **1**. The deprotonated form of the hydrate dpk ligand (dpk-OH)$^-$, of which the bridgehead carbon atom is converted to *gem*-diol by addition of a water molecule to the carbonyl carbon of the dpk ligand, coordinated through a pyridyl N atom and an O atom from the deprotonated *gem*-diol group. The Ag ion had a distorted trigonal geometry with Cl(1)*, Cl(2), and N(2) atoms, and the sum of the angles about the Ag(1) ion was 359.2° (Table 4), i.e., planar geometry. Moreover, the O(1) atom of the (dpk-OH)$^-$ ligand, which coordinated to the Ru ion, also coordinated to the Ag(1) ion as a weakly bound donor (Ag(1)–O(1), 2.576(2) Å), representing coordination number 4 (Table 4). As shown in Fig. 4b,

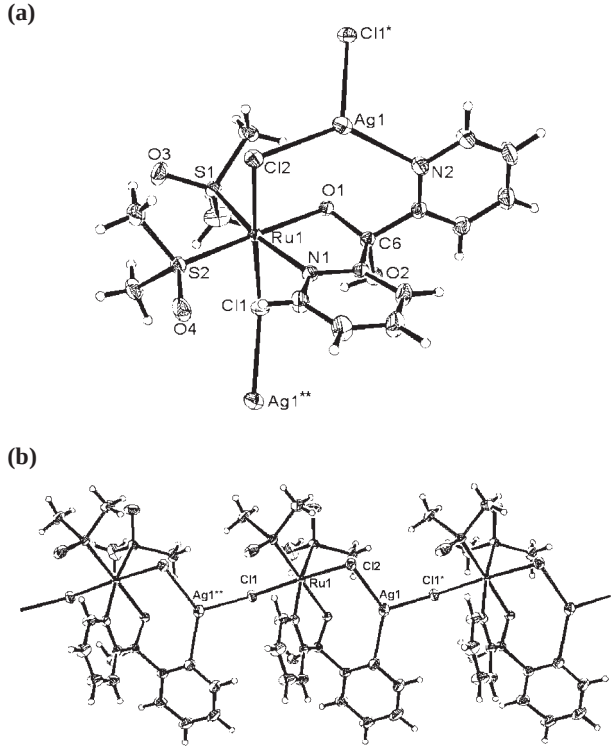

Fig. 4. (a) ORTEP drawing of **3** with 30% probability ellipsoids. (b) View of extended structure of **3**, emphasizing the one-dimensional polymer structure.

Table 4. Selected Bond Lengths, Short Contact (Å), and Angles (°) around Ag in **3**

Bond lengths and short contact/Å		Bond angles/°	
Ag(1)–Cl(2)	2.486(1)	Cl(1)*–Ag(1)–N(2)	107.69(8)
Ag(1)–Cl(1)*	2.531(1)	Cl(1)*–Ag(1)–Cl(2)	118.92(3)
Ag(1)–N(2)	2.262(3)	Cl(2)–Ag(1)–N(2)	132.58(8)
Ag(1)···O(1)	2.576(2)		

the backbone of the polymer was a zigzag [Ag(1)–Cl(2)–Ru(1)–Cl(1)]$_\infty$ chain, in which the N(2) and O(1) atoms of the $(dpk\text{-}OH)^-$ ligand coordinated to Ag(1) on the Cl(2) side. Examples of Ru–Ag coordination polymers with Ag–Cl–Ru–Cl unit have been reported.[45,46] The Ru center was still bound to its original set of ligands; however, the ketone (C=O) was converted to deprotonated *gem*-diol (HO–C–O$^-$). This species is in an "arrested" state of chloride ion abstraction. A similar instance of arrested chloride abstraction has been reported for the reaction of *trans*-[$RuCl_2$(DMeOPrPE)$_2$] (DMeOPrPE = 1,2-bis[bis(methoxypropyl)phosphino]ethane) with $TlPF_6$, in which a one-dimensional polymer containing the Ru complex and a Tl(I) ion is formed.[47]

The obtained C(6)–O(1) and C(6)–O(2) distances (1.367(3) and 1.441(4) Å, respectively) were reasonable for $(dpk\text{-}OH)^-$. The angles about the bridgehead carbon C(6) (110.4(2)–112.1(2)°) indicate sp^3 hybridization of bridgehead carbon C(6). The structural parameters about the Ru(1) ion in **3** were comparable with those of **1**. It is noted that the Ru(1)–O(1) distance (2.105(2) Å) in **3** was similar to that of **1** (2.089(2) Å), although there was a difference in charge between the coordinate O atoms of the $(dpk\text{-}OH)^-$ and dpk ligands.

Inspection of the crystal structure of **3** suggests that the formation of **3** from **1** requires the presence of a Ag^+ and a OH^- ion. Thus, as mentioned in the experimental section, after the addition of Ag^+ to the acidic aqueous solution of **1**, the following addition of OH^- to bring the solution to pH $\approx$ 8 resulted in rapid formation of **3** in good yield (90%, Scheme 2).

Although the Ru–Ag polymer **3** was found to be insoluble in many solvents, it was slightly soluble in DMSO. The ^{1}H NMR spectrum of **3** in DMSO-d_6 exhibited eight signals with intensities of 1H in the aromatic region, four singlets with intensities of 3H in the aliphatic region, and a singlet with intensity of 1H at δ 5.89 (Fig. S6). The aromatic signals were assigned on the basis of the coupling constants and ^{1}H–^{1}H COSY experiments. The singlet at δ 5.89 was assigned to the proton of the *gem*-diol group. The spectral pattern of **3** was similar to that of **1** except a significant upfield H-3 signal at δ 6.48 in **3** (Fig. S7). Judging by the similarity of the spectral patterns,

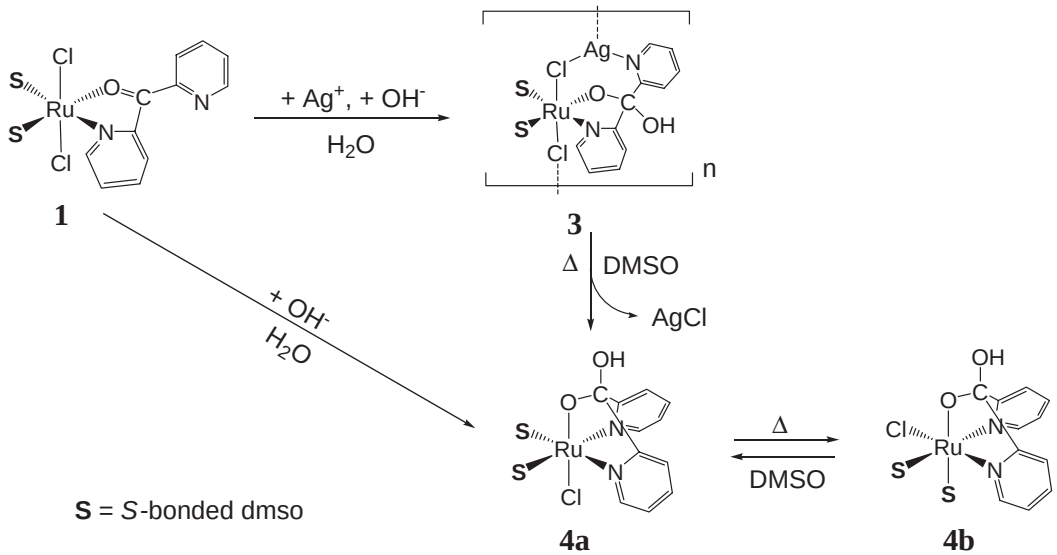

Scheme 2.

the most downfield H-6 signal was assigned to the pyridyl-N(1) ring that coordinated to Ru ion. Thus, the upfield shift of H-3 proton in **3** at δ 6.48, which was comparable to that of corresponding H-3 proton of the coordinate pyridine ring in **1** at δ 9.63, was probably caused by the ring-current effect of the pyridyl-N(2) ring. In crystal structure, the H-3 proton (H(1) atom in X-ray crystal structure) of the pyridyl-N(1) ring was above the pyridyl-N(2) ring. The distance of H-3···centroid of pyridyl-N(2) ring was 3.24 Å, and the perpendicular distance was 2.51 Å in Fig. S8. Therefore, the significant upfield shift of H-3 proton indicates that **3** in DMSO solution retains the Ru–Ag dimer unit as revealed the X-ray crystal structure and H-3 proton is influenced by the ring-current effect of the pyridyl-N(2) ring. When the Ru–Ag coordination polymer **3** was dissolved in DMSO, the Ag(1)–Cl(1)* bonds in the polymer ruptured to form the Ru–Ag dimer *trans*(Cl),*cis*(S)-[AgRuCl$_2$(dpk-OH-κ^3N,O,N')(dmso-S)$_2$].

Synthesis and Structure of *trans*(Cl,O),*cis*(S)-[RuCl(dpk-OH-κ^3N,O,N')(dmso-S)$_2$] (4a). As the Ru–Ag polymer **3** was found to be in an arrested state of chloride abstraction, we attempted to "resolve" the arrested state by further reaction. The reaction of the Ru–Ag polymer **3** in DMSO-d_6 solution was monitored at room temperature by means of NMR spectroscopy. The ^{1}H NMR spectrum of the solution after 3.5 h exhibited the set of five signals for **4a** in addition to the nine signals of **3** (Fig. S7d). Then, a suspension of **3** (0.5 g, 3.8 mmol) in DMSO (25 mL) was heated to 353 K for 30 min. The resulting AgCl precipitate was removed by filtration. After the filtrate was cooled to room temperature, EtOH (25 mL) and diethyl ether (150 mL) were added to precipitate the yellow product (0.32 g, 80%), which was a mixture of geometrical isomers: *trans*(Cl,O),*cis*(S)-[RuCl(dpk-OH-κ^3N,O,N')(dmso-S)$_2$] (**4a**) (≈90%) and a small amount of *cis*(Cl,O),*cis*(S)-isomer (**4b**) (≈10%). Further purification was then necessary. Since the *trans*(Cl,O),*cis*(S)-isomer **4a** in DMSO isomerizes to the *cis*(Cl,O),*cis*(S)-isomer **4b**, as mentioned later, the presence of the minor product **4b** is probably due to isomerization of the *trans*(Cl,O),*cis*(S)-isomer **4a** during heating at 353 K (Scheme 2). To prevent isomerization of **4a** to **4b**, selective synthesis of **4a** was performed without heating; we attempted the reaction of **1** with OH^- in H_2O in the absence of Ag^+. At room temperature, only **4a** was afforded in high yield (≈86%) without the need for further purification (Scheme 2). If a large amount of OH^- ion was used for the reaction, **4a** formed quickly but the isolation of **4a** became difficult because **4a** was more soluble in EtOH in the presence of Li^+ ion.

An ORTEP drawing of **4a** is shown in Fig. 5. The Ru ion had a distorted octahedral geometry with the two *cis*(S) atoms of the two dmso ligands (*cis*(S)-isomer) and the (dpk-OH)$^-$ ligand coordinated in tridentate fashion via two pyridyl N atoms and a *gem*-diol O atom (κ^3N,O,N'), which was *trans* to Cl atom (*trans*(Cl,O)-isomer). Selected bond lengths and angles are listed in Tables 2 and 3, respectively.

The most interesting feature of the structure of **4a** is its *trans*(Cl,O)-geometry. If the reaction of **1** with OH^- is considered frankly, it may be thought that the carbonyl carbon of **1** is attacked by OH^- to yield the deprotonated form of the *gem*-diol (dpk-OH)$^-$, and the non-coordinate pyridyl N atom attacks the axial coordination site of the Cl^- ligand to release the Cl^- ion and allow the N atom to occupy the axial site. Thus, *cis*(Cl,O)-isomer **4b** is formed. However, the X-ray crystal structure of **4a** revealed that the geometry of product is *trans*(Cl,O), and the coordination site of the Cl^- ion in **1** was occupied by the O atom of the *gem*-diol (dpk-OH)$^-$. Experiments to explore the mechanism of κ^3N,O,N'-coordination in the (dpk-OH)$^-$ ligand via NMR spectroscopy are currently underway, and the details will be reported in a separate paper.

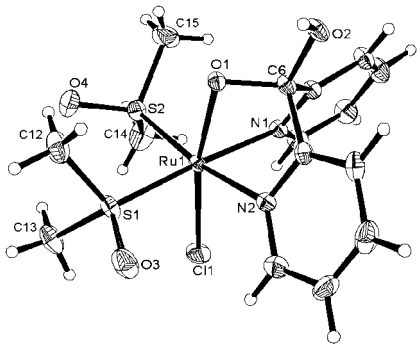

Fig. 5. ORTEP drawing of **4a** with 30% probability ellipsoids.

The *trans*(Cl,O),*cis*(S)-geometry in **4a**, apart from the axial O atom, can be compared with that of *trans*(Cl),*cis*(S)-[RuCl$_2$(Hdpa)(dmso-S)$_2$].[41] The obtained Ru–S distances (av. 2.257 Å) are shorter than those of *trans*(Cl),*cis*(S)-[RuCl$_2$(Hdpa)(dmso-S)$_2$] (av. 2.277 Å) and comparable to those in **1** (av. 2.245 Å), which indicates less steric hindrance among the equatorial ligands compared to that of *trans*(Cl),*cis*(S)-[RuCl$_2$(Hdpa)(dmso-S)$_2$]. The Ru–N distances (av. 2.095 Å) in **4a** are shorter than those of *trans*(Cl),*cis*(S)-[RuCl$_2$(Hdpa)(dmso-S)$_2$] (av. 2.127 Å), which also suggests that the steric effect of the *cis* dmso ligands within the equatorial plane in **4a** is smaller than that found in *trans*(Cl),*cis*(S)-[RuCl$_2$(Hdpa)(dmso-S)$_2$]. The structural parameters of the (dpk-OH)$^-$ ligand in **4a** can also be compared with those of the bis(dpk-OH)$^-$ complex *trans*(O)-[Ru(dpk-OH-κ^3N,O,N')$_2$]·8H$_2$O.[20] The Ru–N distances in **4a** are longer than those of the bis(dpk-OH)$^-$ complex (av. 2.061 Å). The lengthening of the Ru–N bonds of the (dpk-OH)$^-$ ligand is caused by the steric effect of *cis* dmso ligands within the equatorial plane. The steric effect of the *cis* dmso ligands causes reduction of the N(1)–Ru(1)–N(2) bite angle of 82.12(9)° compared with that of bis(dpk-OH)$^-$ complex (94.4(2)°). Moreover, the dihedral angle of the two pyridine rings (74.4(1)°) in **4a** is less than that of the bis(dpk-OH)$^-$ complex (109°); the pyridine rings in **4a** are "folded" due to the steric effect of the equatorial *cis* dmso ligands. However, the structural parameters around the bridgehead C(6) atom (C(6)–O(1) = 1.403(3) Å and C(1)–C(6)–C(7) = 106.1(2)°) were consistent with those of the bis(dpk-OH)$^-$ complex (1.411(6) Å and 106.6(4)°, respectively). The folding of the pyridine rings results in a significantly longer Ru–O distance (2.094(2) Å) compared to that of the bis(dpk-OH)$^-$ complex (1.975(4) Å). The structural features of **4a** suggest that the transformation (pyridine ring folding) of the (dpk-OH)$^-$ ligand results in the lessening of the steric hindrance among the equatorial ligands.

The ^{1}H NMR spectrum of **4a** in DMSO-d_6, shown in Fig. 6,

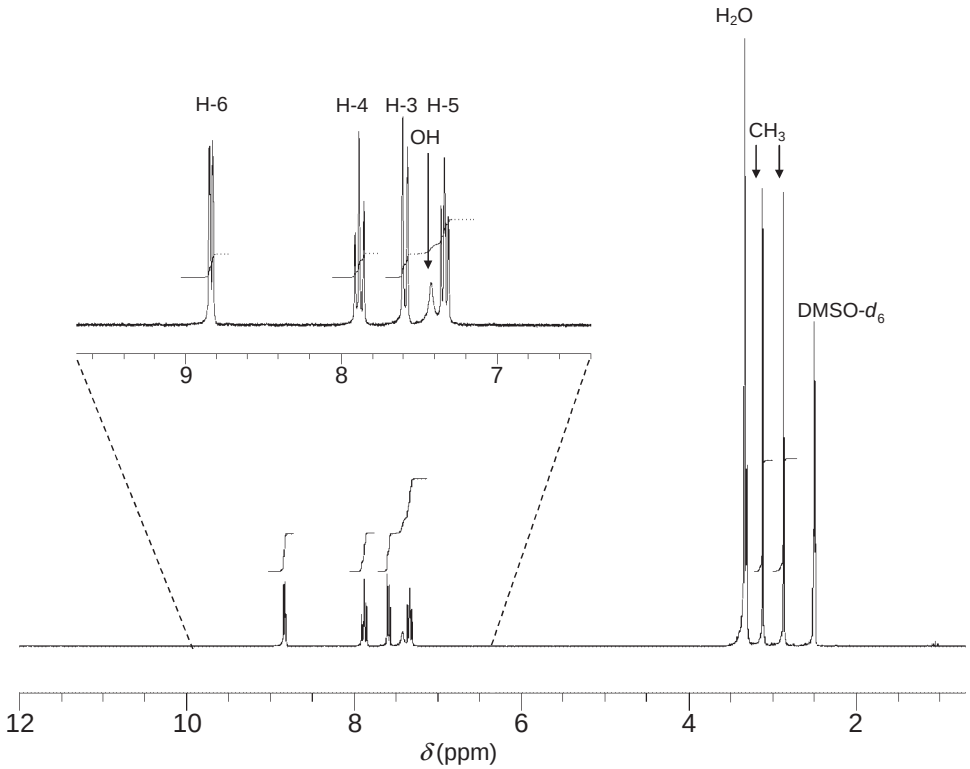

Fig. 6. ^{1}H NMR spectrum of **4a** in DMSO-d_6, recorded at room temperature (298 K).

exhibited four signals with intensities of 2H in the aromatic region, two singlets with intensities of 6H in the aliphatic region, and a broad singlet with intensity of 1H at δ 7.42. The singlet at δ 7.42 was assigned to the proton of the *gem*-diol group. From the signal intensities, **4a** had one (dpk-OH)$^-$ ligand and two dmso ligands. The spectral pattern indicated that the two pyridine rings of the (dpk-OH)$^-$ ligand were equivalent and the two dmso ligands occupied *trans* positions to the two pyridyl N atoms of the (dpk-OH)$^-$ ligand (*trans*(Cl,O),-*cis*(S)-isomer). The aromatic signals were assigned on the basis of coupling constants and ^{1}H–^{1}H COSY experiments. These spectral features were in agreement with the X-ray crystal structure. On the basis of the crystal structure of *trans*-(Cl,O),*cis*(S)-isomer **4a**, the conformation of the two dmso ligands results in different environments for the four methyl groups. This can be explained in terms of the ring-current effect: the methyl-C(12) and -C(13) of the dmso-S(1) ligand are relatively far from the pyridyl-N(2) ring, and their environments (chemical shifts) are similar, while for the dmso-S(2) ligand, the methyl-C(15) is located closer to the pyridyl-N(1) ring than the methyl-C(14), so the proton signal of methyl-C(15) undergoes a greater upfield shift. If the two dmso ligands rotated freely around the Ru–S bonds, the four methyl groups in **4a** should be observed as singlet. However, two methyl signals were observed in the spectrum of **4a** for four methyl groups. Therefore, it is suggested that the two dmso ligands rotate around the Ru–S bonds, but only two equivalent rotamers exist dominantly. One has the same conformation of dmso ligands as observed in the crystal structure, and another is a reverse rotamer, in which the conformation of the two dmso ligands alternates mutually and the methyl-C(13) is located close to the pyridyl-N(2). This situation is equivalent to that of the methyl-C(15) in the former rotamer. The time-averaged spectrum of two rotamers showed a signal for methyl-C(13) and -C(15) at δ 2.87 and a signal for methyl-C(12) and -C(14) at δ 3.12. A similar restricted rotation and rotamers of coordinate dmso ligands in *cis*-[RuCl(bpy)$_2$(dmso-*S*)]-(PF_6)[48] and *cis*(Cl),*cis*(S)-[$RuCl_2$(bpy)(dmso-*S*)$_2$][40] have been reported on the basis of ^{1}H NMR spectroscopy.

Synthesis and Structure of *cis*(Cl,O),*cis*(S)-[RuCl(dpk-OH-κ^3*N*,*O*,*N*′)(dmso-*S*)$_2$] (4b). Isomer **4b** was synthesized via two synthetic methodologies (Scheme 3). Method A was similar to that of **4a**. The reaction of *cis*(Cl),*cis*(S)-dpk-κ^2*N*,*N*′ **2**, instead of *trans*(Cl),*cis*(S)-dpk-κ^2*N*,*O* **1**, with OH$^-$ in H_2O afforded *cis*(Cl,O),*cis*(S)-[RuCl(dpk-OH-κ^3*N*,*O*,*N*′)(dmso-*S*)$_2$] (**4b**). In Method B, the *trans*(Cl,O),*cis*(S)-isomer **4a** was dissolved in DMSO and slowly isomerized to the *cis*(Cl,O),-*cis*(S)-isomer **4b**. Selective precipitation of **4b** over **4a** due to its lower solubility resulted in the high purity of the products. Elemental analysis of **4b** indicated that it had same composition as **4a**, i.e., it was an isomer of **4a**. However, **4b** did not yield crystals suitable for X-ray structural determination, and so, the structure of **4b** was characterized by means of ^{1}H NMR spectroscopy.

The ^{1}H NMR spectrum of **4b** in DMSO-d_6 is shown in Fig. 7; it exhibited eight signals with intensities of 1H in the aromatic region, three singlets with intensities of 3H in the aliphatic region, and a broad singlet with intensity of 1H at δ 7.57. The singlet at δ 7.57 was assigned to the proton of the OH group of the (dpk-OH)$^-$ ligand. The spectral pattern indicates that the two pyridine rings of the (dpk-OH)$^-$ ligand are in different environments, which means that **4b** is an isomer of **4a**, in which the two pyridine rings are in equivalent environments. Therefore, the Cl$^-$ and the dmso ligands occupy

trans positions to the pyridyl N atoms of the $(dpk\text{-}OH)^-$ ligand (*cis*(Cl,O),*cis*(S)-isomer). The aromatic signals were assigned on the basis of coupling constants and ^1H–^1H COSY experiments. Although only three methyl signals out four were observed in DMSO-d_6, it was shown that the remaining methyl signal was obscured by the H_2O signal at δ 3.33. When the spectrum was measured at 373 K, the H_2O signal shifted to δ 2.97, and the fourth signal was observed at δ 3.31 (Fig. S9). The observation of four individual methyl signals suggests that the rotation of the two dmso ligands around the Ru–S bonds is restricted even in DMSO solution. This feature has also been observed in the *cis*(Cl),*cis*(S)-[$RuCl_2$(L-L)(dmso-*S*)$_2$] (L-L = bpy or Hdpa) complexes,[40,41] which have the same geometry of the two dmso ligands as that of *cis*(Cl,O),*cis*(S)-isomer **4b**.

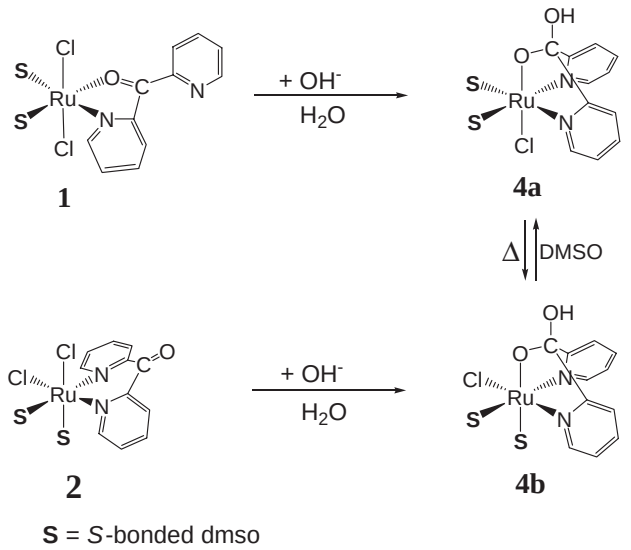

Scheme 3.

Isomerization Reaction between 4a and 4b in DMSO Solution. A DMSO-d_6 solution of *trans*(Cl,O),*cis*(S)-isomer **4a** was sealed in an NMR tube, and the isomerization reaction was monitored at 373 K by means of NMR spectroscopy. The ^1H NMR spectrum of the solution of **4a** after 1 h of heating is shown Fig. 8b, along with the ^1H NMR spectrum taken immediately after dissolution of *trans*(Cl,O),*cis*(S)-isomer **4a** and *cis*(Cl,O),*cis*(S)-isomer **4b** (Figs. 8a and 8c, respectively). In Fig. 8b, it can be seen that although the H-3, H-4, and H-5 signals of two isomers **4a** and **4b** overlap, one signal of **4a** and two signals of **4b**, assigned for H-6 at δ 8.4–9.2, were independently observed. As the reaction proceeded, the signals of *trans*(Cl,O),*cis*(S)-isomer **4a** decreased and the signals of *cis*(Cl,O),*cis*(S)-isomer **4b** increased. After 4 h, an equilibrium was established between **4a** and **4b**, favoring **4b** (K_{4ab} = [**4b**]/[**4a**] = 1.5 ± 0.1). Similarly, when a DMSO-d_6 solution of *cis*(Cl,O),*cis*(S)-isomer **4b** was sealed in an NMR tube and heated at 373 K, the isomerization reaction reached the same equilibrium as when **4a** was used as the starting material (K_{4ab} = 1.5 ± 0.1). Therefore, it was concluded that the isomerization reaction between **4a** and **4b** was reversible.

The reaction rate for the isomerization reaction between *trans*(Cl,O),*cis*(S)-isomer **4a** and *cis*(Cl,O),*cis*(S)-isomer **4b** was determined by ^1H NMR spectroscopy in DMSO-d_6 at

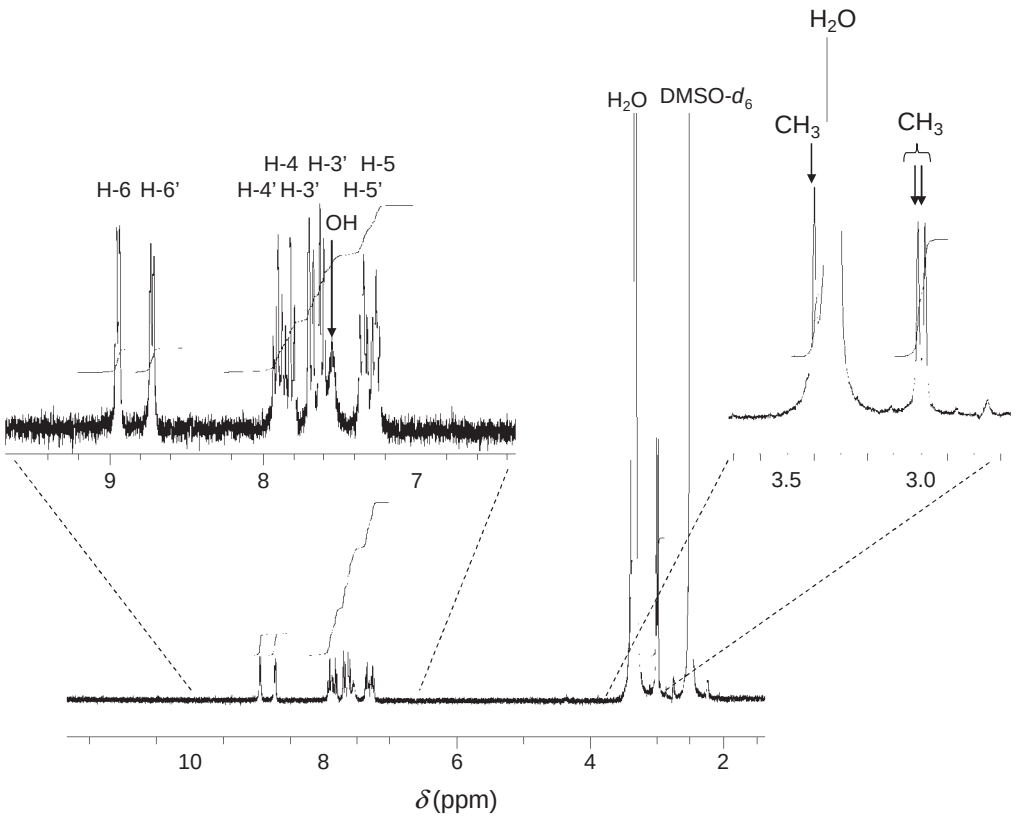

Fig. 7. ^1H NMR spectrum of **4b** in DMSO-d_6, recorded at room temperature (298 K).

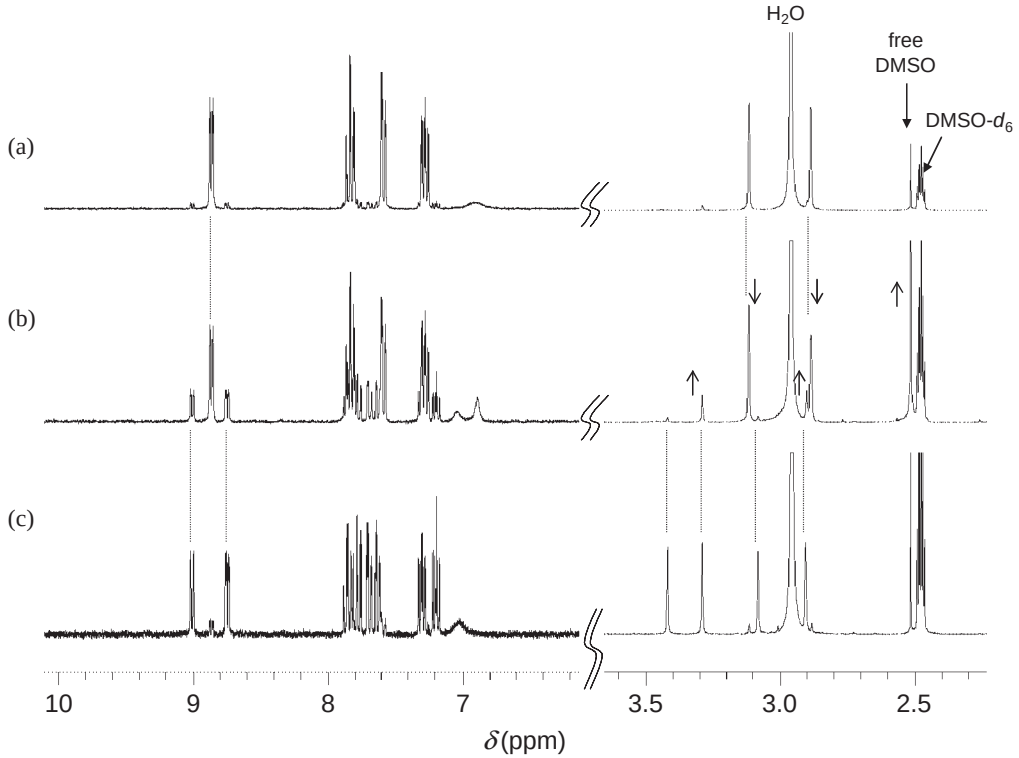

Fig. 8. ^{1}H NMR spectra of **4a** in DMSO-d_6 (a) immediately after dissolution; (b) after 1 h of heating at 373 K. (c) ^{1}H NMR spectrum of **4b** in DMSO-d_6. Spectra were recorded at 373 K.

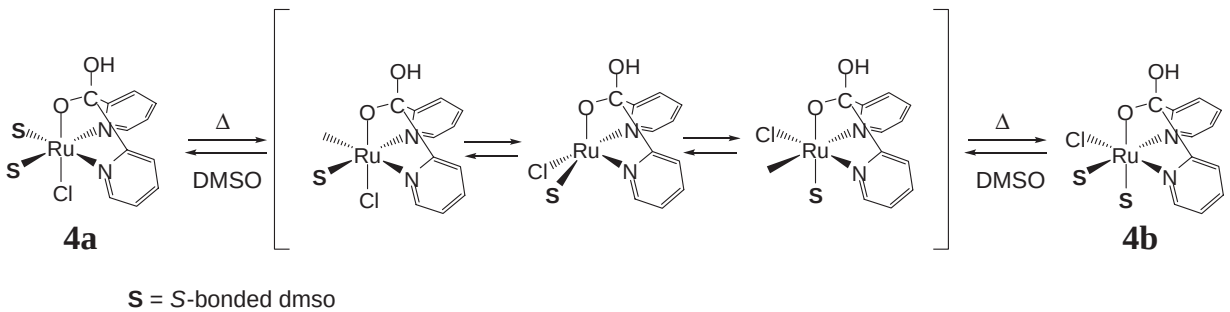

Scheme 4.

373 K. The reaction was monitored over a 5-h period, and the intensities of the H-6 proton signals were normalized with respect to the sum of the intensities of the H-6 proton signals of **4a** and **4b**. After 4 h, an equilibrium was established between **4a** and **4b** with $K_{4ab} = [\mathbf{4b}]/[\mathbf{4a}] = k_{4ai}/k_{-4ai} = 1.5 \pm 0.1$. This system was treated as a reversible first order reaction, and so, the rate constants for the isomerization **4a** $\rightarrow$ **4b** and **4b** $\rightarrow$ **4a** were calculated to be $k_{4ai} = (1.7 \pm 0.1) \times 10^{-4}\,s^{-1}$ and $k_{-4ai} = (1.1 \pm 0.1) \times 10^{-4}\,s^{-1}$, respectively.

During the isomerization reaction, the two dmso signals of **4a** decreased, and the signal of free DMSO and the two of the dmso-ligand signals (δ 3.31 and 2.93) of **4b** increased, but the two methyl signals (δ 3.44 and 3.10) of the other dmso ligand did not appear. In the analogous complex *cis*(Cl),*cis*(S)-[$RuCl_2$(Hdpa)(dmso-S)$_2$], the most upfield methyl signal has been assigned to the methyl group of the axial dmso ligand due to the ring-current effect of the pyridine ring.[41] Therefore, the signals at δ 3.31 and 2.93 can be assigned to the methyl groups of the axial dmso ligand, and the signals at δ 3.44 and 3.10 to the methyl groups of the equatorial dmso ligand. After all, during the isomerization reaction from **4a** to **4b**, only the signals of the axial dmso ligand of **4b** increased. This suggests the existence of a dmso ligand dissociation mechanism for the isomerization reaction between *trans*(Cl,O),*cis*(S)-isomer **4a** and *cis*(Cl,O),*cis*(S)-isomer **4b** in DMSO solution, as shown in Scheme 4. A dissociative mechanism seems reasonable, due to the bulkiness of the dmso ligands, rather than a twist mechanism. The *trans*(Cl,O),*cis*(S)-isomer **4a** releases an equatorial dmso ligand to proceed to the five-coordinate species, and the five-coordinate species isomerize in equilibrium. Re-coordination of solvent DMSO to the five-coordinate species results in the formation of **4a** and **4b**. Therefore, the equatorial dmso ligand in **4b** derives from the solvent, and the axial dmso ligand from the original dmso ligand. When the starting material was **4b**, the signals of the equatorial dmso ligand (δ 3.44 and 3.10) decreased faster than the signals of the

axial dmso ligand (δ 3.31 and 2.93). This also supports that the equatorial dmso ligand in **4b** dissociates to produce the five-coordinate species. In the analogous complex *cis*(Cl),*cis*(S)-[$RuCl_2$(Hdpa)(dmso-*S*)$_2$], the exchange rate of the equatorial dmso ligand was also faster than that of axial dmso ligand.[41] It is thought that due to the characteristic *cis*(Cl),*cis*(S)-geometry, the equatorial dmso ligand is more labile than the axial dmso ligand.

In the previously reported [$RuCl_2$(L-L)(dmso-*S*)$_2$] (L-L = bpy and Hdpa) system, the *trans*(Cl),*cis*(S)-isomer has been shown to be thermodynamically unstable and rearranged to more stable *cis*(Cl),*cis*(S)-isomer.[40,41] The reason for the lower stability of the *trans*(Cl),*cis*(S)-isomer is greater steric hindrance in the equatorial plane, with two dmso-*S* ligands and two pyridyl groups, compared to the *cis*(Cl),*cis*(S)-isomer. Consequently, the isomerization reaction between *trans*(Cl),-*cis*(S)- and *cis*(Cl),*cis*(S)-isomers is irreversible. However, it is worth noting that in this (dpk-OH)$^-$ system, isomerization of the *trans*(Cl,O)- and *cis*(Cl,O)-isomers was reversible without the occurrence of side reactions. The reversibility of isomerization is probably due to the stabilization of *trans*(Cl,O)-isomer **4a**. As mentioned in the discussion of the X-ray crystal structure of **4a**, steric crowding in the equatorial plane, with two dmso-*S* ligands and two pyridyl groups, is mitigated by the transformation (folding up of the pyridine rings) of the (dpk-OH)$^-$ ligand, and so the *trans*(Cl,O)-isomer **4a** becomes similar in stability to *cis*(Cl,O)-isomer **4b**. For a more detailed discussion, the crystal structure of *cis*(Cl,O)-isomer **4b** is required.

Conclusion

Selective syntheses of *trans*(Cl),*cis*(S)-[$RuCl_2$(dpk-κ^2N,O)(dmso-*S*)$_2$] (**1**) and *cis*(Cl),*cis*(S)-[$RuCl_2$(dpk-κ^2N,N')(dmso-*S*)$_2$] (**2**) were carried out, and their crystal structures are reported. In *trans*(Cl),*cis*(S)-Cl_2(dmso-*S*)$_2$, steric effects favor the slimmer κ^2N,O-coordination mode and prevent adoption of the κ^2N,N'-coordination mode. The smaller steric effects in *cis*(Cl),*cis*(S)-Cl_2(dmso-*S*)$_2$ allow adoption of both κ^2N,O- and κ^2N,N'-coordination modes.

The reaction of **1** with Ag^+ and OH^- afforded the one-dimensional Ru–Ag coordination polymer *trans*(Cl),*cis*(S)-[$AgRuCl_2$(dpk-OH-κ^3N,O,N')(dmso-*S*)$_2$]$_n$ (**3**). The X-ray crystal structure of **3** revealed that (dpk-OH)$^-$ coordinates to the Ru^{2+} ion through a pyridyl N atom and an O atom from the deprotonated *gem*-diol group, with the remaining pyridyl N atom coordinated to the Ag^+ ion. The backbone of the polymer consists of a zigzag [–Ag(1)–Cl(2)–Ru(1)–Cl(1)–]$_\infty$ chain. This species was in an "arrested" state of abstraction of a Cl^- ion. Further reaction in DMSO resolved the arrested state and afforded a mixture of two isomers with dpk-OH-κ^3N,O,N'. The major product was *trans*(Cl,O),*cis*(S)-[RuCl(dpk-OH-κ^3N,O,N')(dmso-*S*)$_2$] (**4a**), and the minor product was *cis*-(Cl,O),*cis*(S)-isomer **4b**, which was probably afforded by isomerization of **4a** due to heating at 353 K.

The *trans*(Cl,O),*cis*(S)-isomer **4a** was also selectively synthesized by the reaction of **1** with OH^- in H_2O. The *trans*-(Cl,O),*cis*(S)-isomer **4b** was synthesized by reaction of **2** with OH^- in H_2O. The two isomers **4a** and **4b** underwent interconversion in DMSO solution, with **4b** favored over **4a** in the equilibrium state ($K_{4ab} = 1.5 \pm 0.1$).

Dichlorobis(dimethyl sulfoxide-*S*)ruthenium(II) and chlorobis(dimethyl sulfoxide-*S*)ruthenium(II) complexes containing the dpk ligand in three coordination modes (κ^2N,O-, κ^2N,N'-, and κ^3N,O,N'-) were synthesized. The geometry of the $RuCl_2$(dmso-*S*)$_2$ unit causes selective formation of either the κ^2N,O- or the κ^2N,N'-coordination mode of the dpk ligand. If the $RuCl_2$(dmso-*S*)$_2$ unit is modified to form a RuCl-(dmso-*S*)$_2^+$ unit using OH^-, both the κ^2N,O- and κ^2N,N'-coordination modes of the dpk ligand can convert to the κ^3N,O,N'-coordination mode of the (dpk-OH)$^-$ ligand. Experiments exploring the interconversion between the κ^2N,O- and κ^2N,N'-coordination modes of the dpk ligand, and the formation mechanism and reverse conversion of the κ^3N,O,N'-coordination mode of the (dpk-OH)$^-$ ligand are currently underway.

This work was financially supported by Research Project Grant (B) of the Institute of Science and Technology, Meiji University.

Supporting Information

The absorption spectra of **1**, **2**, **4a**, and **4b** in H_2O (Fig. S1), ^{1}H NMR spectra of **1** in DMSO-d_6 after *t* h of heating at 323 K ($t = 0$, 2, 4, and 16 h) (Fig. S2), ^{1}H NMR spectrum of **2** in DMSO-d_6 after 16 h of heating at 323 K (Fig. S3), ^{1}H NMR spectrum of **2** in DMSO-d_6 (Fig. S4), ^{1}H NMR spectrum of **2** in $CDCl_3$ (Fig. S5), ^{1}H NMR spectrum of **3** in DMSO-d_6 (Fig. S6), ^{1}H NMR spectrum of **1** and ^{1}H NMR spectra of **3** in DMSO-d_6 after *t* h at room temperature ($t = 0$ and 3.5 h) (Fig. S7), Space-filling model of **3** (Fig. S8), and ^{1}H NMR spectrum of **4b** in the aliphatic region in DMSO-d_6 recorded at 373 K (Fig. S9) are in PDF format. This material is available free of charge on the web at http://www.csj.jp/journals/bcsj/.

References

1 A. Juris, V. Balzani, F. Barigelletti, S. Campagna, P. Belser, A. von Zelewsky, *Coord. Chem. Rev.* **1988**, *84*, 85.
2 V. Balzani, A. Juris, M. Venturi, S. Campagna, S. Serroni, *Chem. Rev.* **1996**, *96*, 759.
3 F. Barigelletti, L. Flamigni, *Chem. Soc. Rev.* **2000**, *29*, 1.
4 T. J. Meyer, *Pure Appl. Chem.* **1986**, *58*, 1193.
5 M. K. Nazeeruddin, C. Klein, P. Liska, M. Grätzel, *Coord. Chem. Rev.* **2005**, *249*, 1460.
6 M. Grätzel, *Coord. Chem. Rev.* **1991**, *111*, 167.
7 S. Ito, P. Liska, P. Comte, R. Charvet, P. Péchy, U. Bach, L. Schmidt-Mende, S. M. Zakeeruddin, A. Kay, M. K. Nazeeruddin, M. Grätzel, *Chem. Commun.* **2005**, 4351.
8 C. R. Rice, M. D. Ward, M. K. Nazeeruddin, M. Grätzel, *New J. Chem.* **2000**, *24*, 651.
9 F. Liu, G. J. Meyer, *Inorg. Chem.* **2005**, *44*, 9305.
10 Y.-Y. Lü, L.-H. Gao, M.-J. Han, K.-Z. Wang, *Eur. J. Inorg. Chem.* **2006**, 430.
11 G. Yang, S.-L. Zheng, X.-M. Chen, H. K. Lee, Z.-Y. Zhou, T. C. W. Mak, *Inorg. Chim. Acta* **2000**, *303*, 86.
12 C. Godard, S. B. Duckett, S. Parsons, R. N. Perutz, *Chem. Commun.* **2003**, 2332.
13 K. N. Crowder, S. J. Garcia, R. L. Burr, J. M. North, M. H. Wilson, B. L. Conley, P. E. Fanwick, P. S. White, K. D. Sienerth, R. M. Granger, II, *Inorg. Chem.* **2004**, *43*, 72.
14 M. Bakir, J. A. M. McKenzie, *J. Chem. Soc., Dalton Trans.*

1997, 3571.

15 J. Madureira, T. M. Santos, B. J. Goodfellow, M. Lucena, J. P. de Jesus, M. G. Santana-Marques, M. G. B. Drew, V. Félix, *J. Chem. Soc., Dalton Trans.* **2000**, 4422.

16 L. Spiccia, G. B. Deacon, C. M. Kepert, *Coord. Chem. Rev.* **2004**, *248*, 1329.

17 S. Sarkar, B. Sarkar, N. Chanda, S. Kar, S. M. Mobin, J. Fiedler, W. Kaim, G. K. Lahiri, *Inorg. Chem.* **2005**, *44*, 6092.

18 C. M. Kepert, G. B. Deacon, N. Sahely, L. Spiccia, G. D. Fallon, B. W. Skelton, A. H. White, *Inorg. Chem.* **2004**, *43*, 2818.

19 G. B. Deacon, C. M. Kepert, N. Sahely, B. W. Skelton, L. Spiccia, N. C. Thomas, A. H. White, *J. Chem. Soc., Dalton Trans.* **1999**, 275.

20 S. Sommerer, W. P. Jensen, R. A. Jacobson, *Inorg. Chem. Acta* **1990**, *172*, 3.

21 X. Zhou, D. C. R. Hockless, A. C. Willis, W. G. Jackson, *J. Mol. Struct.* **2005**, *740*, 91.

22 Z. Serna, M. G. Barandika, R. Cortés, M. K. Urtiaga, M. I. Arriortua, *Polyhedron* **1998**, *18*, 249.

23 J. M. Seco, M. Quirós, M. J. G. Garmendia, *Polyhedron* **2000**, *19*, 1005.

24 M.-L. Tong, S.-L. Zheng, J.-X. Shi, Y.-X. Tong, H. K. Lee, X.-M. Chen, *J. Chem. Soc., Dalton Trans.* **2002**, 1727.

25 W. L. Huang, J. R. Lee, S. Y. Shi, C. Y. Tsai, *Trans. Met. Chem.* **2003**, *28*, 381.

26 C. G. Efthymiou, C. P. Raptopoulou, A. Terzis, R. Boča, M. Korabic, J. Mrozinski, S. P. Perlepes, E. G. Bakalbassis, *Eur. J. Inorg. Chem.* **2006**, 2236.

27 J. Grewe, A. Hagenbach, B. Stromburg, R. Alberto, E. Vazquez-Lopez, U. Abram, *Z. Anorg. Allg. Chem.* **2003**, *629*, 303.

28 F. Zhang, M. E. Broczkowski, M. C. Jennings, R. J. Puddephatt, *Can. J. Chem.* **2005**, *83*, 595.

29 F. Zhang, E. M. Prokopchuk, M. E. Broczkowski, M. C. Jennings, R. J. Puddephatt, *Organometallics* **2006**, *25*, 1583.

30 A. P. Martínez, M. P. García, F. J. Lahoz, L. A. Oro, *Inorg. Chim. Acta* **2003**, *347*, 86.

31 A. Caballero, M. C. Carrión, G. Espino, F. A. Jalón, B. R. Manzano, *Polyhedron* **2004**, *23*, 361.

32 B. Binotti, C. Carfagna, E. Foresti, A. Macchioni, P. Sabatino, C. Zuccaccia, D. Zuccaccia, *Organomet. Chem.* **2004**, *689*, 647.

33 S. Pal, S. Pal, *Acta Crystallogr., Sect. C* **2002**, *58*, m273.

34 D. L. Reger, J. R. Gardinier, M. D. Smith, P. J. Pellechia, *Inorg. Chem.* **2003**, *42*, 482.

35 D. Zuccaccia, G. Bellachioma, G. Cardaci, C. Zuccaccia, A. Macchioni, *Dalton Trans.* **2006**, 1963.

36 S. L. Queiroz, A. A. Batista, M. P. de Araujo, R. C. Bianchini, G. Oliva, J. Ellena, B. R. James, *Can. J. Chem.* **2003**, *81*, 1263.

37 G. Bellachioma, G. Cardaci, V. Gramlich, A. Macchioni, M. Valentini, C. Zuccaccia, *Organomellics* **1998**, *17*, 5025.

38 A. S. A. T. de Paula, B. E. Mann, E. Tfouni, *Polyhedron* **1999**, *18*, 2017.

39 E. Alessio, G. Mestroni, G. Nardin, W. M. Attia, M. Calligaris, G. Sava, S. Zorzet, *Inorg. Chem.* **1988**, *27*, 4099.

40 M. Toyama, K. Inoue, S. Iwamatsu, N. Nagao, *Bull. Chem. Soc. Jpn.* **2006**, *79*, 1525.

41 M. Toyama, R. Suganoya, D. Tsuduura, N. Nagao, *Bull. Chem. Soc. Jpn.* in press.

42 The formal name of **1** is (*OC*-6-14)-[$RuCl_2$(dpk-κ^2N,O)-(dmso-S)$_2$], that of **2** being (*OC*-6-32)-[$RuCl_2$(dpk-κ^2N,N')(dmso-S)$_2$], that of **3** being (*OC*-6-14)-[$AgRuCl_2$(dpk-OH-κ^3N,O,N')-(dmso-S)$_2$]$_n$, that of **4a** being (*OC*-6-34)-[RuCl(dpk-OH-κ^3N,O,N')-(dmso-S)$_2$], and that of **4b** being (*OC*-6-44)-[RuCl(dpk-OH-κ^3N,O,N')(dmso-S)$_2$].

43 I. P. Evans, A. Spencer, G. Wilkinson, *J. Chem. Soc., Dalton Trans.* **1973**, 204.

44 *teXsan Crystal Structure Analysis Package*, Molecular Structure Corporation, **1992**.

45 L. Carlucci, G. Ciani, F. Porta, D. M. Proserpio, L. Santagostini, *Andew. Chem., Int. Ed.* **2002**, *41*, 1907.

46 A. Vertova, I. Cucchi, F. Porta, D. M. Proserpio, S. Rondinini, *Electrochim. Acta* **2006**, in press.

47 N. K. Szymczak, F. Han, D. R. Tyler, *J. Chem. Soc., Dalton Trans.* **2004**, 3941.

48 D. Hesek, Y. Inoue, S. R. L. Everitt, H. Ishida, M. Kunieda, M. G. B. Drew, *J. Chem. Soc., Dalton Trans.* **1999**, 3701.